Journal of Applied Polymer Science

Electrospun protective self-healing coatings for light alloys: A better understanding of the intrinsic potential of the technology

Amin Firouzi, Andrea Impagnatiello, Costantino Del Gaudio, Francesca Romana Lamastra, Alessandra Bianco, Giampiero Montesperelli

Department of Enterprise Engineering "Mario Lucertini", University of Rome Tor Vergata, INSTM UdR Roma Tor Vergata, Viale del Politecnico, 00133 Rome, Italy

Correspondence to: G. Montesperelli (E-mail: montesperelli@stc.uniroma2.it)

ABSTRACT: Polymeric coating systems exhibit high potentiality to provide an effective barrier against corrosion of metallic surfaces. However, these coatings can lose their protective characteristics because of their high susceptibility to damage. Thus, the addition of corrosion inhibitors is desirable and considered as an alternative route for active corrosion protection. In the present work, eco-friendly electrospun coatings of poly(vinyl alcohol) (PVA) loaded with cerium salts have been deposited onto aluminium 6082 alloy. Two different precursors of cerium (III) (*i.e.*, cerium nitrate and cerium acetylacetonate) were added to the electrospinning solutions and the effectiveness of the resulting nanofibrous coatings was evaluated for the healing of generated defects. The microstructural features of the electrospun coatings have been investigated by scanning electron microscopy, infraredspectroscopy, and thermal analysis. Tensile tests were performed to assess the mechanical properties of the different fibrous coatings. The electrochemical behavior of both intact and damaged coatings was evaluated in 3 wt % NaCl solution by means of electrochemical impedance spectroscopy. All the deposited PVA coatings loaded with cerium(III) salts showed remarkable corrosion resistance. In the case of artificially damaged coatings, a self-healing effect, which stops the development of the corrosion process and provides a significant recovery of the corrosion resistance, has been observed only for coatings loaded with cerium III acetylacetonate. The release of cerium from damaged PVA fibers has been demonstrated by means of inductively coupled plasma mass spectrometry. The observed self-healing effect has been ascribed to the formation of cerium hydroxide on the defective zone, which hindered the corrosion process. © 2015 Wiley Periodicals, Inc. J. Appl. Polym. Sci. **2015**, *132*, 42728.

KEYWORDS: coatings; electrospinning; fibers

Received 3 March 2015; accepted 14 July 2015

DOI: 10.1002/app.42728

INTRODUCTION

Aluminium and its alloys are cost-effective production materials characterized by excellent properties (*i.e.*, light weight, high specific strength-to-weight ratio, and high thermal conductivity), that make them suitable for widespread applications such as heat exchangers, automotive industry, aerospace components, marine, and shore applications.[1–6] However, the potential of these materials can be seriously limited by corrosion attack, especially in aqueous electrolytes containing chlorides, that leads to huge economic losses. Therefore, there is a strong demand for surface treatments or coatings to provide long-lasting anti-corrosion performances.[1,3,7–9]

Several surface treatments or coatings have been conventionally adopted to improve the corrosion protection of metal alloys. These include electrochemical plating,[10] anodizing,[11–15] and chemical conversion coating.[12,14,16,17] Some cases of these processes still rely on the use of chromates. In recent years, because of the high toxicity of chromium compounds, health and environmental concerns have led to the progressive discontinuation of such treatments.[1,18] Nowadays, organic coatings are extensively used to impart corrosion resistance because of their (i) good barrier characteristics, (ii) ability to include active anti-corrosion pigments, such as corrosion inhibitors, and (iii) low manufacturing costs. Several authors have investigated corrosion protection of organic coatings on Al alloys.[1–3,7,8,19–21] Nevertheless, the mechanical properties of organic coating systems are not comparable to those of metallic substrates, as coating layers can be easily damaged or scratched by mechanical impacts during transportation, installation, or service, thus losing their protective features.[9,19] The most common types of defects might affect the protective and aesthetic properties of a coating system are superficial mechanical damage, substrate-reaching mechanical damage, delamination at the defective zone, and local delamination.

So far, if some of the mentioned defects occur, thus compromising the coating efficiency and eventually exposing the substrate, a manual repair or a replacement of the damaged part is required. However, the detection of internal damages is very challenging and a manual intervention may be expensive and in some cases even impossible.

Hence, in the last years, design and development of new organic coatings with self-healing properties have become an important target for many industries. Currently, two main strategies are followed in order to deal with an effective self-healing organic coating. On one hand, polymeric coatings able to recover their barrier effect rather than their integrity by gap filling have been designed. In this case, the aim is to fill the damaged volume *via* the release of reactive liquids from containers incorporated within the bulk of the coating. On the other hand, the most common approach deals with free-moving corrosion inhibitors released from the coating systems. If a scratch exposes the metallic surface, the corrosion inhibitor diffuses towards the damaged site to induce metal passivation. This healing methodology also works in intact organic coatings, since water and oxygen diffusion through the coating is a matter of time thus requiring an active corrosion protection to occur.[19,22,23] An early example of a self-repairing organic system was presented by White *et al.*,[24] the idea was to incorporate a microencapsulated healing agent and an embedded solid-phase catalyst within a structural polymeric material. Later, different types of self-healing systems have been reported including those based on microcapsules embedment,[24–27] reversible chemistries[28,29], and hollow fibers embedment.[30,31] In this regard, electrospinning technique is a flexible, cost-effective, easily exploitable process able to provide **long, continuous fibers form the micro- down to the nano-scale.** The range of materials covers soluble artificial polymers such as polyvinyl alcohol, through to natural polymers, such as proteins and polysaccharides. Electrospun fibers are produced in a continuous length, giving a notable advantage over other nano-scale fibers only available in micron lengths.

Peculiar properties of these fibrous products predispose them for very promising applications**. In fact,** electrospinning offers several advantages such as control over morphology, porosity, and composition using a rather simple equipment. A very high surface area to volume ratio can be achieved making them ideal for any application that depends on having a large surface area (e.g. catalysts, bioreactor substrates, active filtration). Moreover, because of the mechanism of fiber formation, e-spun polymeric fabrics are characterized by a high draw ratio. This potentially can result in a high degree of molecular alignment, which would allow the fiber to attain a high tensile strength, making them extremely suitable for the fabrication of nanocomposites. Finally, the typical microstructure of electrospun fiber mats, in terms of nanoscale fiber diameter and voids among fibers in a mesh, make them appropriate for specific applications in the fields of tissue engineering and ultra-filtration. Main disadvantages of the elecrospinning process include the large number of interdependent variables (i.e. solution parameters, ambient parameters, process parameters), and eventually the use of hazardous solvents. Some years ago also the low production rate was also of concerns. However, presently, there is considerable growth in this emerging field with the availability of plants both at industrial scale and as laboratory scale. Self-healing coatings can be readily deposited to large area substrates in a continuous process. Recently, Liu *et al.*[32] proposed a new delivery system as healing agent based on the electrospinning technique, encapsulating the moisture reactive precursor $TiCl_4$ within the pores of collected poly(lactic acid) (PLA). Electrospun PLA fibers are reactive to the atmospheric water, eliciting the hydrolysis of the polymer structure and thus the release of the reactive metal oxide precursor. Braun *et al.*[33] employed the coaxial electrospinning encapsulation method to fabricate self-healing polymer coating systems. Using this approach, polysiloxane precursor, the healing agent, was fed through the inner capillary to be encapsulated into a core-shell bead-on-string electrospunfibers of a poly(vinylpyrrolidone) sheath, which was fed through the outer capillary. A defect to the coating allowed to release the healing agent into the damaged site and to activate the subsequent protection of the underlying substrate from corrosion. Interestingly, salts of rare earth (RE) elements were found to have self-healing capability for aluminium alloys.[34–36] They control the cathodic reaction by precipitating metal hydroxide at the defects since oxygen reduction in the damaged area leads to a local increase of pH value because of the generation of OH^- ions.[2,3,18,37] Cerium exhibits the highest anticorrosion efficiency among all RE compounds.[3] Hinton and Wilson[38] reported that, the cerium ionis as effective as the chromium ion. The main characteristic that allows cerium to act as an excellent inhibitor agent is related to the formation of Ce^{+4} at high pH values in aerated chloride environments.[3,39]

In this work, we present a potential coating system using conventional electrospinning technique to protect an aluminium alloy 6082 against corrosion in 3 wt % sodium chloride medium. This can be regarded as a straightforward and cost-effective approach to collect a dry coating onto a metallic surface able to overcome the possible limitations associated to coventional deposition techniques. Some of them, such as dip-coating, are based on the direct contact of the polymeric solution with the metallic substrate to protect, thus eventually triggering the corrosion of the substrate itself. The barrier ability of electrospun poly(vinyl alcohol) (PVA) mats containing different cerium compounds (*i.e.*, cerium (III) nitrate and cerium (III) acetylacetonate) was investigated by means of electrochemical impedance spectroscopy. Polyvinyl alcohol is a linear synthetic polymer obtained *via* partial or full hydrolysis of polyvinyl acetate, the amount of hydroxylation determining physical characteristics, chemical properties, and mechanical properties. It is an environmental friendly, water-soluble polymer with excellent film forming property, and emulsifying properties and outstanding resistance to oil, grease, and organic solvents. Because of these overall features, PVA is commonly used for textile and paper manufacturing. Moreover, PVA exhibits also outstanding barrier properties and excellent biocompatibility that makes it suitable for food packaging and for a number of different biomedical devices currently available on the market.[40,41]

The self-healing ability of cerium-loaded electrospun coatings was then evaluated by intentionally damaging the collected PVA

Table I. Electrospinning Parameters and Conditions ofThermal Treatment forCe-Loaded PVA Electrospun Coatings

Sample	Cerium precursor	Feed rate (ml/h)	Voltage (kV)	TCD[a] (cm)	Thermal treatment
S0-1	Cerium acetylacetonate (*organic*)	0.4	11	12	-
S1					120°C—60 min
S2					150°C—15 min
S0-2	Cerium nitrate (*inorganic*)		13.7	10	-
S3					120°C—60 min
S4					150°C—15 min

[a] TCD = Tip-to-collector Distance

mat using a knife-edge. So far, and to the best of our knowledge, no clear successful results have been reported to self-heal the damaged site of aluminium alloy using cerium as an inhibitor released from electrospunfibers.

EXPERIMENTAL

Materials

PVA powder (99+% hydrolyzed, $M_w = 130{,}000$ *Sigma-Aldrich*), Triton X-100, glyoxal (40 wt % in H_2O), and cerium (III) acetylacetonate hydrate ($Ce(C_5H_7O_2)_3.xH_2O$,)were supplied by *Sigma-Aldrich*. Cerium (III) nitrate hexahydrate ($Ce(NO_3)_3{\cdot}6H_2O$)was supplied by *Fluka*.

All materials and reagents were used as received.

Preparation of Electrospun Polymeric Coatings

The substrate material used for the current investigation was aluminium alloy 6082. The chemical composition of the alloy is Si (0.7–1.3%wt), Fe (0.5%wt), Cu (0.1%wt), Mn (0.4–1.0%wt), Mg (0.6–1.2%wt), Zn (0.2%wt), Ti (0.25%wt), Cr (0.25%wt), Al (balance).

Samples (18 mm diameter and 1.5 mm thickness) were polished using SiC grit papers. The grinded samples were then cleaned in ethanol, rinsed in distilled water and finally dried in air.

PVA powder was dissolved in deionized water at 80–90°C to prepare 8 wt % aqueous solutions. After cooling the solution to room temperature, Triton X-100 (1 wt %) and glyoxal (10 wt % with respect to PVA) were added as nonionic surfactant and cross-linking agent, respectively. Subsequently, after constant stirring for 24 h at room temperature, a set of polymeric solutions were prepared by adding two different cerium (III) precursors as corrosion inhibitors: cerium (III) nitrate hexahydrate (inorganic compound) or cerium (III) acetylacetonate hydrate (organic compound). The amount of both precursors was 5 wt % with respect to PVA in both cases.

Fibrous coatings were directly deposited onto circular substrates *via* electrospinning technique at constant feed rate and applied voltage by means of a digitally controlled syringe pump (*KD 130 Scientific, USA*) and a high voltage power supply (*Spellman, USA*). Finally, electrospun PVA coatings were thermally treated into an oven in order to activate the cross-linking reaction. For this aim, several procedures were considered selecting different temperatures and curing times, the two most promising ones were then chosen: 120°C—60 min and 150°C—15 min.

Table I summarizes all the investigated electrospinning conditions and thermal treatment parameters.

Characterization Techniques

Viscosity measurements were carried out at 30°C by means of a digital viscometer (*Brookfield DV-II+, Middleboro, USA*) equipped with a spindle SC4–21 rotating at 20 rpm. Electric conductivity was measured by using the CDM230 meter (*Radiometer Analytical, France*) calibrated with a 0.01D KCl solution (1408 μS/cm) at 25°C. All the measurements were repeated three times.

Scanning electron microscopy (SEM; *LEO Supra 35*) coupled with energy dispersive spectroscopy (EDS) (*INCAx-sight, Oxford instruments*) was performed to evaluate the surface of the coated samples.

Thermal properties of the collected mats (i.e., the melting temperature T_m and melting enthalpy ΔH_m) were assessed by differential scanning calorimetry (DSC) (*Netzsch DSC 200PC*), considering the first heating scan in the following conditions: N_2 atmosphere, heating rate of 10°C/min, temperature range 20–265°C. The crystallinity degree of the electrospun samples was calculated as follows:[40,42]

$$X_c = \frac{\Delta H_m}{\Delta H_m^0} 100$$

where ΔH_m^0 is the melting enthalpy of 100% crystalline PVA (138.6 J/g).[40,43]

Fourier transform infrared (FTIR) spectrometer (*Nicolet 3700, Thermo Fisher Scientific*) was used for chemical analysis of electrospun PVA mats using attenuated total reflection accessory with ZnSe prism. Spectra were acquired in the range of 4000–400 cm^{-1}, 256 scans were performed for each specimen at a resolution of 4 cm^{-1}.

The mechanical characterization was performed by means of uniaxial tensile tests on dog-bone specimens cut out from the electrospun mats (ASTM D 1708; testing length 22.25 mm, width 4.8 mm). For this aim, a universal testing machine (*Lloyd LRX*) equipped with a 100 N load cell was used to test the here considered samples up to rupture at 1.2 mm/min. The tensile modulus (E), the stress at break (σ_{max}) and the strain at break (ε_f) were calculated from the acquired stress-strain curves, considering the nominal cross-sectional area of the specimens. Four specimens were tested for each electrospun mat.

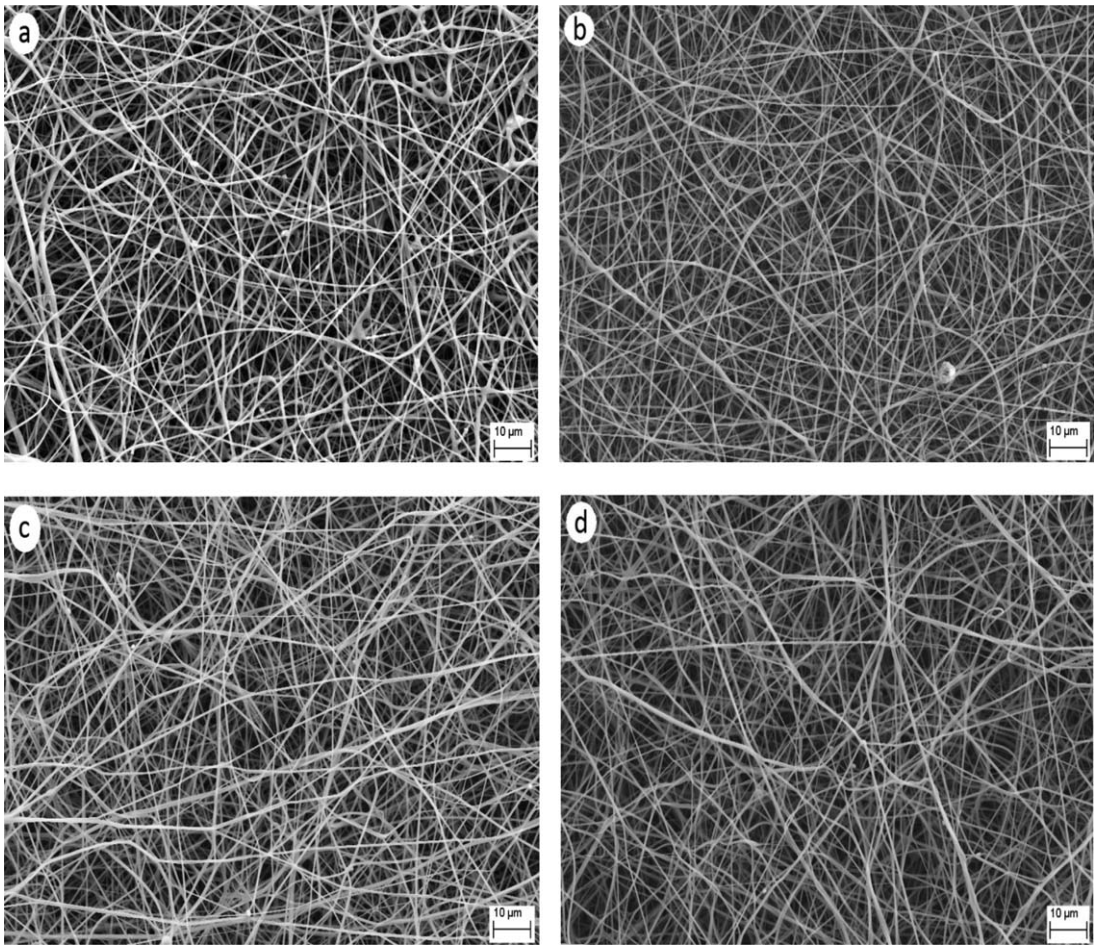

Figure 1. SEM micrographs of thermally treated PVA electrospun mats loaded with organic cerium and treated at 120°C (a) and 150°C (b); SEM micrographs of electrospun mats loaded with inorganic cerium and treated at 120°C (c) and (d) 150°C.

The anti-corrosion properties of bare and polymer coated samples were assessed by electrochemical impedance spectroscopy (EIS) using a 1260 Solartron Frequency Response Analyzer and a 1287 Solartron Electrochemical Interface in 3% NaCl solution at room temperature. An alternate signal, 10 mV in amplitude, was applied at the open circuit potential in the frequency range $10^{-2}-10^{5}$ Hz. A three-electrode setup, consisting of a platinum counter electrode, a saturated Ag/AgCl reference electrode and the investigated sample ($\sim$ 1.5 cm^2) as a working electrode, was used. Data were collected and analyzed by Zplot-Zview softwares *(Scribner Associates Inc.)*.

Finally, the actual amount of cerium released at room temperature from the different fibrous mats in the chosen corrosive environment (*i.e.*, 3% NaCl solution), was evaluated by means of inductively coupled plasma mass spectrometry (ICP-MS) (*Agilent 7500 series*).

The adhesion strength of Ce-loaded PVA electrospun coatings on the substrate was evaluated as follows. The specimen was fixed to the sample stage of a universal testing machine (UTM, *Lloyd LRX*) equipped with a 50 N load cell, a piston was mounted on the movable cross head of the UTM. Then, a double side adhesive was placed onto the sample surface. A compressive preload to ensure a good bonding of the piston to the coating was applied for 5 s. Finally, a tensile load was applied at 3 mm/min until the coating removal. Four specimens were tested for each kind of sample.

RESULTS AND DISCUSSION

Properties of the e-Spun Solutions: Viscosity and Conductivity

Results of viscosity and electrical conductivity of the solutions prepared for electrospinning showed that the presence of either cerium nitrate or cerium acetylacetonate in the solution resulted in increased viscosity from 1315 to 1560 and 1760 mPa·s, respectively. Also, the conductivity increased from 2.79 ± 0.01 to 3.72 ± 0.01 and 5.05 ± 0.02 mS/cm for solutions containing organic and inorganic cerium salts, respectively.[45,46]

Characterization of PVA Electrospun Mats: SEM, DSC, and FTIR

SEM micrographs of cross-linked electrospun PVA mats loaded with cerium inhibitors are shown in Figure 1. The obtained electrospun mats containing organic cerium were comprised of randomly arranged fibers free of defects with smooth surface, fairly uniform diameter and highly interconnected architecture. The average fiber diameters were 410 ± 80 nm and 420 ± 80 nm

Table II. Thermal and Mechanical Properties of all the E-Spun Fibrous PVA Coatings

	Thermal			Mechanical		
Sample	T_m (°C)	ΔH_m (J/g)	X_c (%)	E (MPa)	σ_{max} (MPa)	ε_f (%)
S0-1	220.3	59.67	43.05	38±8	2.1±0.2	89±16
S1	206.0	37.45	27.02	30±10	2.4±0.6	64±11
S2	217.4	53.04	38.27	66±12	5.2±0.9	56±13
S0-2	212.3	64.53	46.56	51±10	4.4±0.3	122±8
S3	196.9	23.52	16.97	31±5	2.1±0.5	48±10
S4	208.2	12.87	9.28	90±16	6.9±1.5	48±4

for samples thermally treated at 120°C—60 min and 150°C—15 min, respectively [Figure 1(a,b)].

In the case of inorganic cerium, fabrication of electrospun mats was not successful since electrospraying was the dominant process. Thus, in order to collect reliable electrospun mats, different Triton amounts between 0 and 2 wt % were considered. It resulted that the most suitable condition was 0.5 wt %. For samples derived from this latter solution, the average fiber diameters were 450±100 nm (at 120°C—60 min) and 470±110 nm (at 150°C—15 min) [Figure 1(c,d)].[45,47] Furthermore, especially in the case of inorganic cerium, the high conductivity of the solution (5.056 ± 0.019 mS/cm) gave rise to a broader diameter distribution compared to that including organic cerium (3.721 ± 0.010 mS/cm).[45]

Melting temperature (T_m), melting enthalpy (ΔH_m), and crystallinity degree (X_c) of electrospun PVA mats were determined by DSC, results were summarized in Table II. Thermally treated PVA mats at 120°C and 150°C containing either organic or inorganic cerium showed significant decrease in the melting temperature and crystallinity degree compared to as-spun (without treatment) mats (i.e., 220°C and 43% for S0–1 and 212°C and 46% for S0–2, respectively). Previous studies[48–50] have reported that the activation of the cross-linking reaction resulted in lower crystallinity degree accompanied by decreased melting temperatures. The X_c values of the electrospun mats containing organic cerium were about 27% and 38% for S1 and S2 samples, respectively. Conversely, inorganic cerium contributed to lower the X_c value down to 17% and 9% for S3 and S4 samples, respectively. Moreover, a significant difference in the X_c has been recorded among samples treated at 120°C and 150°C. These results are in good agreement with Refs. 48,49, the degree of cross-linking being inversely related to the X_c value and increasing with the time and temperature of the cross-linking reaction.

The ATR-FTIR spectra of electrospun PVA mats containing either organic or inorganic cerium are presented in Figure 2. According to the literature,[51] all the samples showed the same absorption bands at 3300, 2940, 2900, 1420, 1330, 1250, 1140, 1090, and 850 cm^{-1}. In details, the peaks at 3300 and 1330 cm^{-1} correspond, respectively, to the O–H *stretching* mode and to the HC-OH *bending* mode. The two absorptions around 2940 and 2900 cm^{-1} have to be attributed to asymmetrical and symmetrical C-H *stretching*, respectively. Bands at 1420 and 850 cm^{-1} are associated to the *bending* vibrations of CH_2 groups, *wagging* and *rocking*, respectively. Moreover, the C-C *stretching* in crystalline and amorphous regions was detected at 1140 and 1250 cm^{-1}, respectively. Finally, the band at 1090 cm^{-1} has to be assigned to C-O *stretching* of neat PVA. It is worth to point out that, usually, cross-linking reactions of PVA with dialdehydes result in a broader absorption band in

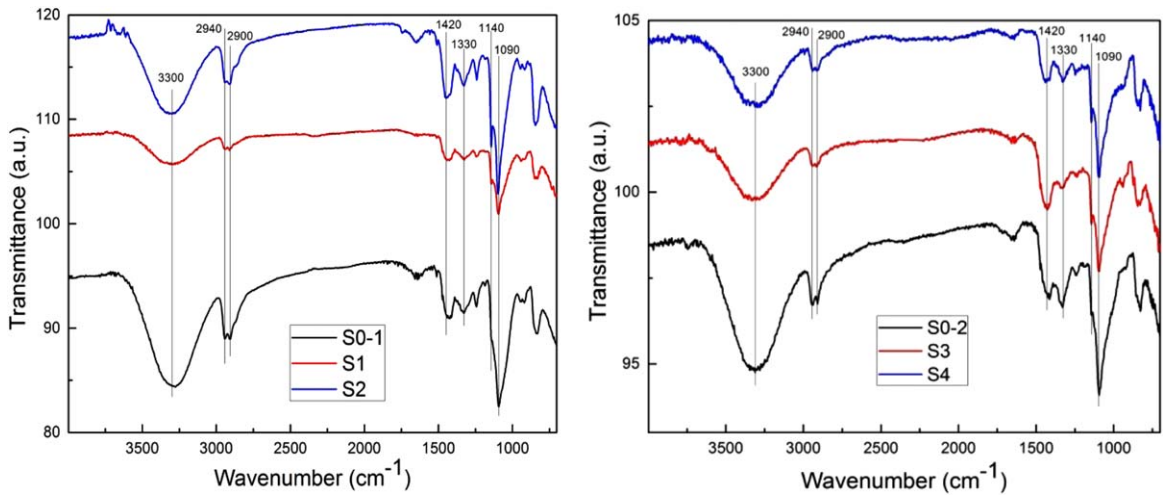

Figure 2. FTIR spectra of as-spun and thermally treated PVA mats loaded with organic cerium (left panel) and inorganic cerium (right panel). [Color figure can be viewed in the online issue, which is available at wileyonlinelibrary.com.]

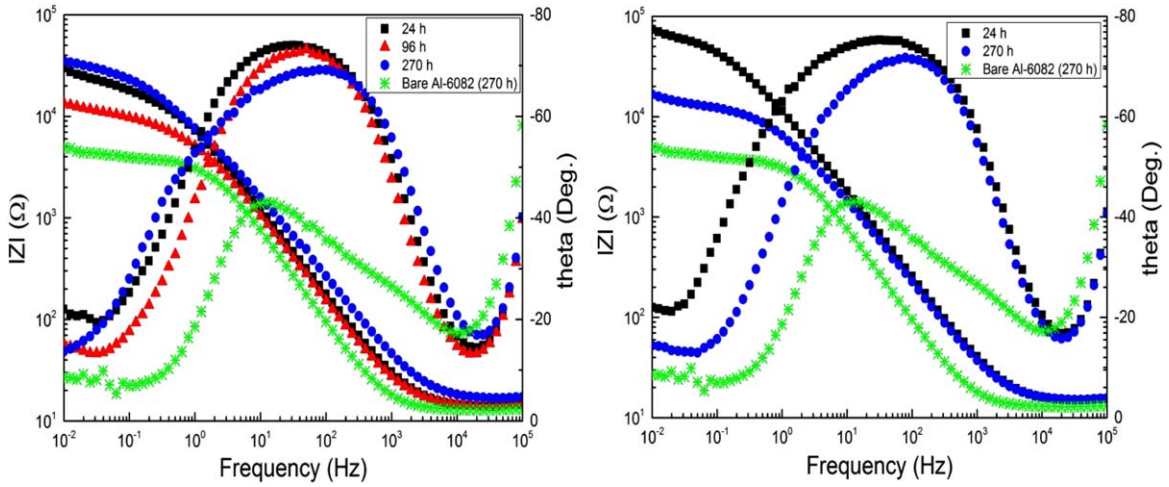

Figure 3. EIS spectrum of sample S1 (left panel) and sample S2 (right panel) in Bode representation (EIS spectra of bare metallic substrate after 270 h immersion are reported for comparison). [Color figure can be viewed in the online issue, which is available at wileyonlinelibrary.com.]

the range 1000–1140 cm^{-1}, attributed both to C-O and C-O-C vibrations. In this case, this occurrence has not been detected, probably because of the low cross-linking degree.

Mechanical Characterization of As-Spun and Cross-Linked PVA Mats

Mechanical properties of electrospun fibrous mats as resulted from the uniaxial tensile tests are resumed in Table II. The values of the tensile modulus were 30±10 and 66±12 MPa, the stress at break was 2.4±0.6 and 5.2±0.9 MPa for S1 and S2 coatings, respectively. Moreover, strain at break of cross-linked mats assumed values significantly smaller than that measured for as-spun (S0–1) mat, as expected. According to previous studies,[48,52,53] cross-linking improves the mechanical properties and an effective modification of this characteristic can be obtained by performing a thermal treatment in oven at 150°C (i.e., S2).

For electrospun mats containing inorganic cerium, analogous results were obtained. As a general trend, samples treated at 150°C (S4) recorded higher mechanical properties compared to those recorded at 120°C (S3), demonstrating again that also in this case an effective cross-linking can be obtained in the former condition.

For all of the investigated electrospun coating (S1, S2, S3, and S4), the adhesion test showed that a tensile load of about 10 N causes delamination, leaving a thin layer still adhering to the substrate. Therefore, the actual adhesion strength of the electrospun coating on the substrate can be considered higher than 10 N. This value seems not *significantly affected neither by cross-linking conditions nor by the nature of the loaded* cerium *(III)* salt.

It is well known that the adhesion strength of organic coatings strictly depends on the metal/coating system and occurs either mechanically or chemically. In the mechanical adhesion, the coating penetrates the surface in its defects establishing a bond, which can be improved by increasing its roughness. On the other hand, the chemical adhesion occurs at the metal/organic coating interface when interatomic bonds take place. Metal/polymer interfacial bonds are generally secondary or hydrogen bridge type. Poor adhesion exerts strong influence on the corrosion protection of a metallic surface and can be caused by different factors, such as excessive film thickness or insufficient superficial cleaning. Poor adhesion allows the electrolyte to diffuse more easily into the region between the surface and the coating, finally leading to film detachment.

EIS Assessment of the Coating Systems

EIS is one of the most extensively used nondestructive techniques which provides quantitative information on corrosion resistance of coating systems.[18,54,55] Acquired data can be evaluated through an equivalent circuit whose electrical response is representative of the electrochemical behavior of the substrate-coating system. It is well known that the EIS spectrum of a coated sample is given by the contribution of coating properties (coating capacitance C_{coat} and pore resistance R_{pore}) in the high frequency region and faradaic processes (charge transfer resistance R_{ct} and double layer capacitance C_{dl}) in the low frequency region.[19,56] In this work, the coating thickness is not an issue, but the impedance of the coating is the figure of merit. EIS measurements were carried out at room temperature to evaluate the barrier and active anticorrosion performance of electrospun PVA coatings containing cerium inhibitors onto the Al-6082 alloy during immersion in 3 wt % NaCl corrosive environment.

Barrier Ability of Polymeric Coatings. Evolution of Bode plots for the S1 and S2 coating systems are shown in Figure 3. Very high impedance (close to 67 kΩ) was recorded after 24 h immersion of S2 in 3 wt % NaCl corrosive medium, while it was about 21 kΩ for S1. At immersion time longer than 24 h, a different behavior was observed. The impedance of S1 slowly decreased to the value of about 11 kΩ after 96 h immersion, as the electrolyte begins to reach the surface of metallic substrate. Then, a remarkable increase of impedance at all frequencies occurred, being 35 kΩ after 270 h which exceeded that of the sample initially immersed in solution for 24 h, whereas in the case of S2, its value drastically decreased to about 12 kΩ after the same immersion period. These results will be further discussed in "Quantitative

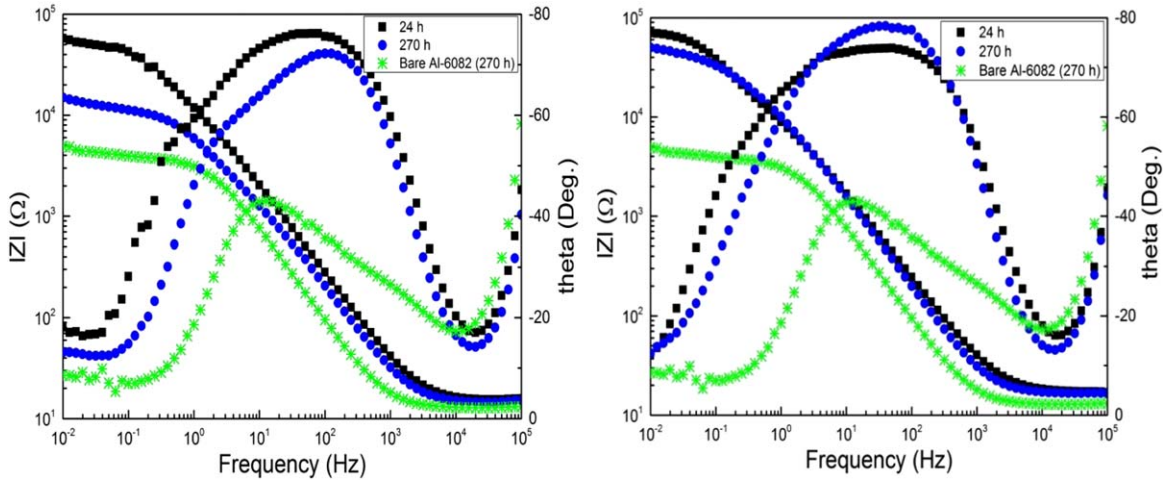

Figure 4. EIS spectrum of sample S3 (left panel) and sample S4 (right panel) in Bode representation (EIS spectra of bare sample after 270 h immersion are reported for comparison). [Color figure can be viewed in the online issue, which is available at wileyonlinelibrary.com.]

Analysis of Cerium Released from the E-Spun Coating Systems in the corrosive environment" section where the amount of inhibitor released from fibrous coatings was measured by ICP-MS. The electrochemical test was also performed on bare Al-6082 (not coated) for direct comparison and the resistance value was only 3.8 kΩ after 270 h immersion.

Figure 4 shows EIS plots of S3 and S4 coatings in Bode representation after immersion in an aqueous NaCl solution (EIS spectra of bare sample after 270 h immersion are also reported for direct comparison). An initial impedance of about 52 kΩ was recorded after 24 h immersion for S3 sample. Then, the impedance dramatically decreased to 13 kΩ for longer exposure time up to 270 h. On the other hand, S4 showed very high initial impedance after 24 h immersion (about 58 kΩ), which slightly lowered at about 54 kΩ after 270 h, the highest value recorded among all the intact coatings after 270 h immersion.

The trend of phase as a function of frequency in Figures 3 and 4 clearly reveals the presence of two time constants whose role will be discussed later.

SEM micrographs of all the coating systems after electrochemical tests are shown in Figure 5. It can be observed that the S3 coating broke up during the test [see inset in Figure 5(c)]. This result can be ascribed to an ineffective cross-linking procedure, as previously observed. Mechanical tests confirmed this point and, in addition, led to a critical discussion of DSC measurements. According to the observation here reported, it can be suggested that inorganic cerium-hindered PVA chain rearrangement, thus decreasing the crystallinity degree. Therefore, even if cross-linking usually contributes to decrease X_c, this is strictly verified for neat PVA treated with glyoxal under proper thermal conditions. The obtained result seems to demonstrate that the presence of inorganic cerium negatively affected the final performance of the electrospun mat, being characterized by an inadequate resistance against breakdown in NaCl solution.

Self-Healing Ability of Polymeric Coatings. EIS measurements were also carried out to evaluate the self-healing ability of the coating systems. Considering the results reported in the previous section, only the self-healing properties of the S1 and S4 coatings, which have excellent barrier ability, were investigated in 3 wt % NaCl solution. Here, the samples were damaged by scratching the surface before immersion. For this aim, a razor blade was used, giving a scratch width of about 40 μm, which penetrated down to the substrate as confirmed by SEM (see Figure 7). Depending on the used inhibitor (organic or inorganic), two types of results were obtained. In the case of scratched S4 sample, no modification was observed and EIS diagrams did not give satisfactory results, see Figure 6(a). The impedance value progressively decreased and a remarkable drop occurred from 58 kΩ after 24 h immersion to 18 kΩ after 270 h immersion. Since the substrate is not covered by the coating anymore because of the presence of the defect, the faradaic process was intensified and consequently the low frequency range of the diagram is affected by the defect. On the other hand, for scratched S1 sample, EIS diagram is modified and an increase of both modulus and phase angle has been measured in the both high and low frequency ranges. For a better explanation of this phenomenon, the corresponding Bode diagram is plotted in Figure 6(b). After 4 himmersion, a high impedance value of about 238 kΩ was measured that remarkably decreased to about 25 kΩ after 24 h. However, after this stage, the impedance has been recovered and its value progressively increased at about 74 kΩ after 96 h immersion. Then, the resistance continued to increase at all frequencies and reached a considerable value of about 82 kΩ after 270 h immersion, characterized by a broad phase angle which suggests that the substrate was progressively sealed off with the consequent increase of the charge transfer resistance. EIS measurements were also carried out for scratched control sample (i.e., without inhibitor) for the same immersion period in order to have a comparison with the treated sample. Resistance of the sample decreased with the immersion time without any recovery. The ongoing depression of the impedance value during the whole immersion period may be induced by the development of corrosion process in the defective zone [see Figure 6(c)]. The remarkable different electrochemical behavior of the self-healing and control samples undoubtedly confirms the effectiveness of the here proposed approach to include cerium acetylacetonate within

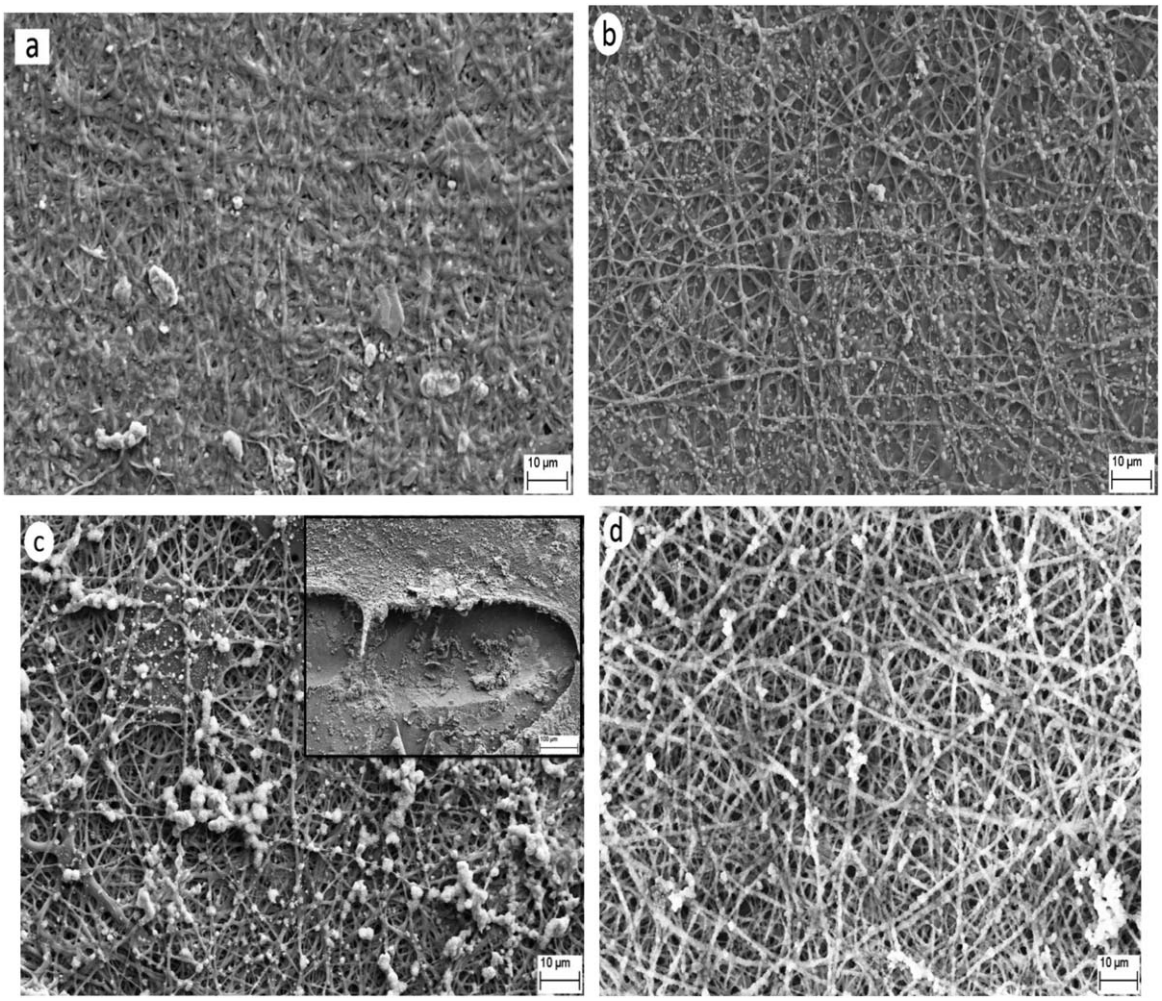

Figure 5. SEM micrographs of the electrospun PVA coating systems after the electrochemical test: (a) sample S1, (b) sample S2, (c) sample S3, and (d) sample S4. Inset magnification in panel (c) shows the coating break up during the performed electrochemical test.

PVA fibers as an effective agent to inhibit corrosion. SEM micrographs of the damaged region after electrochemical tests are illustrated in Figure 7. After aqueous NaCl solution immersion for 270 h, no evidence of corrosion was observed on the self-healing sample (scratched S1) while the control sample corroded in the scribed area [Figure 7(a,b)].

It is well known, that corrosion is due because of the coupling of two galvanic elements, in which the corroding metal is the anodic component. In our system, the aluminum alloy is oxidized by oxygen, according to the following reactions:

$$Al \rightleftharpoons Al^{3+} + 3e^{-} \quad (1)$$

$$O_2 + 4H^{+} + 4e^{-} \rightleftharpoons 2H_2O \quad (2)$$

The reaction (2) consumes H^{+} ions and produces a local pH increase.

Inhibitors are a large class of chemicals able to slow down the rate of the cathodic and/or anodic reaction following different mechanisms. The accepted inhibition mechanism of cerium salts passes through the oxidation of Ce(III) to Ce(IV) caused by hydrogen peroxide, which is produced from the cathodic reaction of oxygen reduction:[3,18,37,57]

$$O_2 + 2H_2O + 2e^{-} \rightarrow H_2O_2 + 2OH^{-} \quad (3)$$

The generated peroxide can in turn oxidize Ce(III) by the following reaction, forming cerium hydroxide:

$$Ce^{3+} + H_2O_2 + 2OH^{-} \rightarrow Ce(OH)_4 \quad (4)$$

Cerium hydroxide is insoluble and precipitates on the cathodic site of the metal surface on which reaction (2) mainly occurs. This restricts the metal contact with the environment, reducing the occurrence of the corrosion reaction.

In our samples, the released Ce^{3+} ions gradually diffused from broken fibers to bare Al-6082 surface and react according (4); consequently, a cerium hydroxide layer is formed on the defective zone. This passive layer can cover the corroded area thus hindering the corrosion process, exhibiting the "self-healing" capability. EDS mapping of cerium on scratched S1 sample confirmed this possible healing mechanism [Figure 7(e)]. The samples were then stored in an ambient condition for 8 months after immersion in aqueous NaCl solution for 270 h. Interestingly, no evidence of corrosion was again observed on the scratched S1 sample while the scratched control sample exhibited extensive corrosion [Figure 7(c,d)].

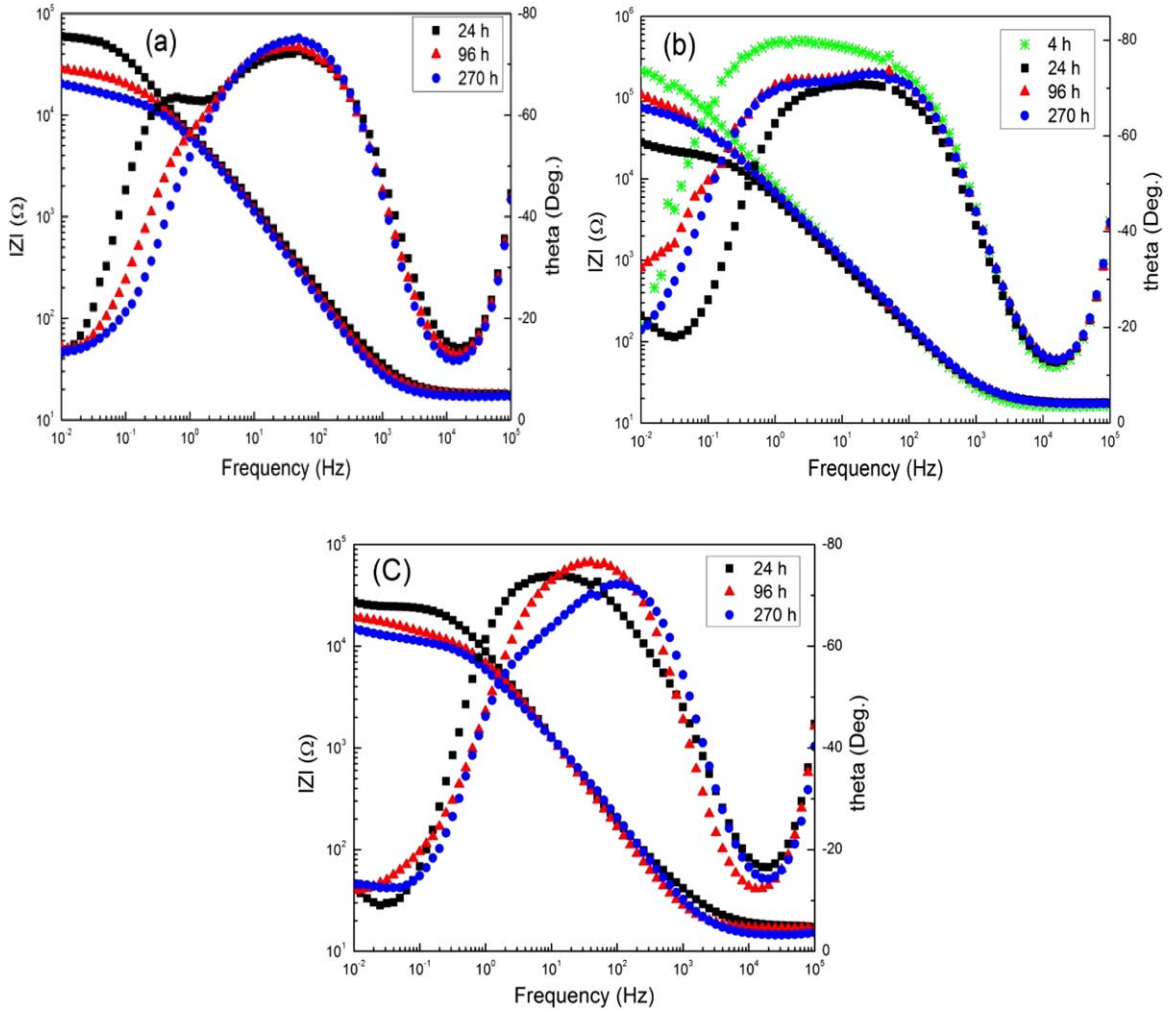

Figure 6. EIS spectrum of artificially damaged coatings: (a) sample S4, (b) sample S1, and (c) control without cerium in Bode representation. [Color figure can be viewed in the online issue, which is available at wileyonlinelibrary.com.]

For quantitative estimation of the anticorrosion performance of the coating systems in 3 wt % NaCl solution, experimental data were fitted using equivalent circuit models as shown in Figure 8. For intact coatings (S1–S4), the classical equivalent circuit, presented in Figure 8(a), was selected.[19,56,58] This model was established considering the following characteristics: R_{sol} characterized the solution resistance, CPE_{coat} and R_{pore} referred to the capacitance and resistance of the electrospun fibrous coating, whileR_{ct} in parallel with CPE_{dl} represented the charge transfer resistance and double layer capacitance originated from faradaic process present at the substrate/coating interface. Here, the constant phase elements (CPE) have been used instead of a real capacitance to take into account the nonideal behavior of the sample resulting from nonuniformity of the coatings.[18,56,59]

The coating systems exhibited high resistance at early exposure time to NaCl solution since the electrolyte can hardly penetrate through the pores of the coating. Longer immersion time (up to 24 h) resulted in the coating saturation and eventually, the chloride ions reached the substrate-coating interface resulting in a decrease of R_{pore} value. At this stage, the corrosion protection of the substrate is mainly attributed to the good barrier capability of the coating.[18,59] Hence, experimental data (up to 24 h) could properly be simulated using the model shown in Figure 8(b) except for sample S3 where two time constants were clearly observed after 24 h immersion. The formation of ionically conducting pathways was expanded after 24 h of immersion, and the electrolyte finally interacted with the substrate and the corresponding equivalent circuit is depicted in Figure 8(a). Figure 9 shows an example of the fitting results obtained on the spectrum of the intact S1 and S4 coatings after 270 h immersion, in Bode representation, using the equivalent circuit of Figure 8(a). A perfect agreement between experimental and numerical data was obtained as χ^2 test values were lower than 10^{-4} which means that the circuit model is well adapted to the experimental system.

Considering that processes taking place on an artificially damaged sample are different from those of an intact coating, different circuit model should be proposed for the scratched samples. Hence, we used another equivalent circuit for the coating with the macro defect presented in Figure 7.[19] Here, the CPE_{coat} was replaced by a pure capacitance C_{coat}. The presence of the defect

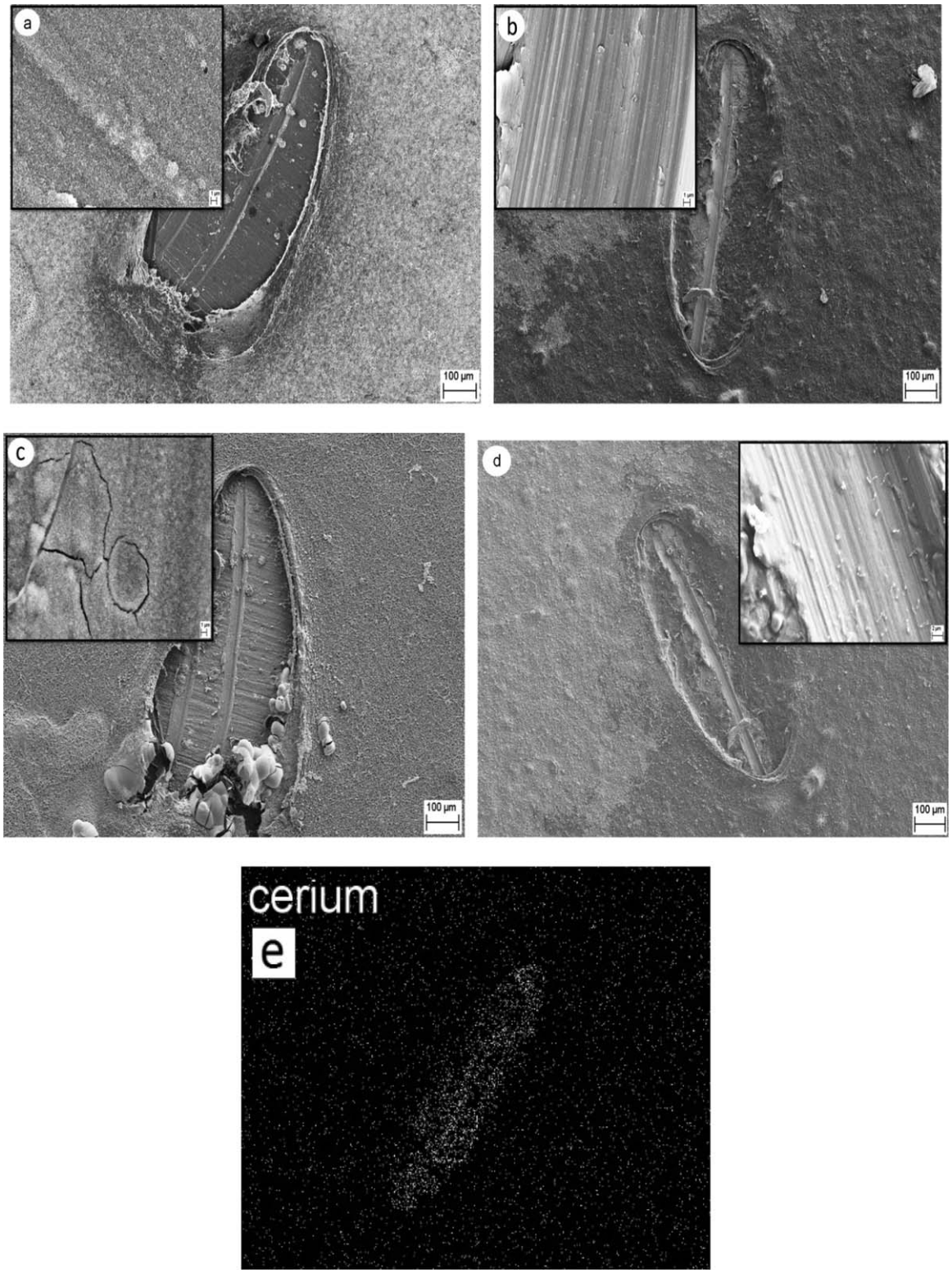

Figure 7. SEM micrographs of artificially damaged coatings after corrosion test: (a) control (without cerium), (b) sample S1, (c) and (d) stored (a) and (b) in an ambient condition for 8 months, respectively (inset magnifications show the scratch surface), (e) EDS mapping of cerium on (b).

masked the nonideal behavior of the coating.[19] In addition, a new phenomenon occurred in the defective zone, a time constant related to the passive layer, which was characterized by a resistance($R_{passive}$) and a capacitance($CPE_{passive}$). Figure 9(c) shows an example of the fitting of the EIS spectrum of the scratched S1 after 270 h immersion, using the equivalent circuit of Figure 8(c). The χ^2 test confirmed this assumption, computing a value lower than 10^{-4}.

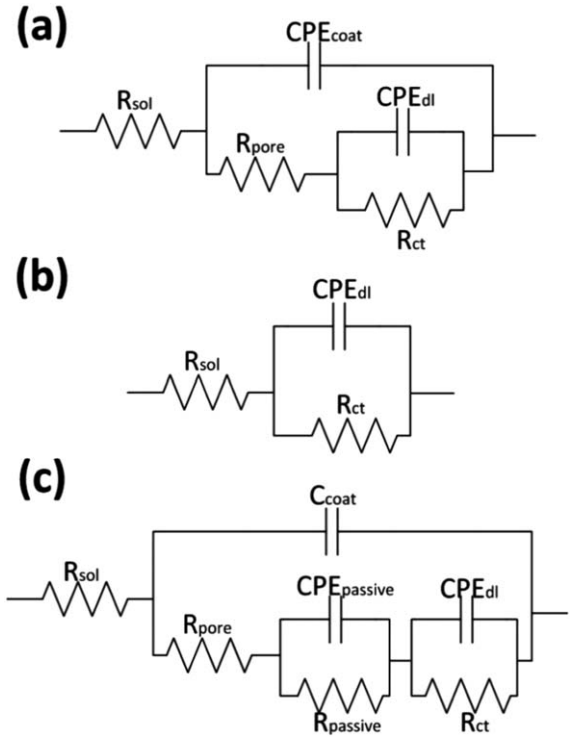

Figure 8. Representative equivalent circuits of the e-spun coatings used for the EIS data fitting: (a) intact coatings after 24, (b) intact coating up to 24 h, and (c) damaged coatings.

The effects of the healing agents on the charge transfer resistance of the scratched S1 and S4 as a function of time are summarized in Figure 10. As a comparison, a control sample (PVA intact coating without Ce) has been also reported.The decrease of the corrosion resistance at the beginning for all the samples could indeed be related to the electrolyte diffusion into the electrospun fibrous coating. After about 120 h immersion, samples demonstrated a relatively stable behavior. As reported before, the self-healing effect could only be observed when the cerium III acetylacetonate (Scratched S1) was used. In this case, the final R_{ct} was about one order of magnitude higher than that of the control sample (without healing agent) while using cerium III nitrate, an effective healing process did not occur. However, additional experiments are necessary to explore the different behavior in the Ce release mechanism from the electrospun fibrous mats. It will be an objective of the future work.

Quantitative Analysis of Cerium Released from the E-Spun Coating Systems in the Corrosive Environment

ICP-MS measurements were carried out on the corrosive environment to evaluate the amount of inhibitor released from either intact or damaged coatings.Results are reported in Table III. In the case of the intact coating S1, a significant amount of cerium (i.e. 0.2 μg/L) was recorded. On the other side, for the intact coating S2, the amount of cerium eventually released in the soaking solution was not detectable. These results supported the electrochemical tests. In fact, it can be suggested that after 24 h immersion, the electrolyte containing Cl^- ions reached the substrate and resulted in local delamination. The pH increase, as a consequence of cathodic reaction in the defective zone, stimulates the inhibitor to be released but it takes time in the absence of a damage. Thus, the impedance recovery of the intact coating S1 after 96 h was because of the gradual cerium release from the fibrous coating. On the other side, the impedance value of the intact coating S2 progressively decreased because of the development of corrosion phenomenon underneath the coating in absence of fast inhibitor release. This different behavior provides a clear evidence of an easier Ce release mechanism from sample S1 with respect to sample S2. In the case of intact coatings containing inorganic cerium, similar inhibitor amount (i.e., around 0.1 μg/L) was recorded for both S3 and S4 coatings. Interestingly, the amount of cerium released from artificially damaged coating S1 confirms the possible self-healing mechanism described earlier (Self-Healing Ability of Polymeric Coatings section). In the case of damaged S1 and S4 coatings, the measured amount of released cerium was 0.5 and 0.1 μg/L, respectively. Remarkable cerium release from damaged S1 resulted in self-healing functionality of the coating. Regarding damaged S4, the absence of cerium release contributed to the progressive impedance decrease. The different response observed for the here proposed systems has somehow to be related to the coating itself, considering that a number of independent variable might affect the releasing process such as thickness, cross-linking degree, crystallinity as well as the chemical nature of the loaded cerium salt.

CONCLUSION

Presently, the applications of electrospun fabrics are widely growing especially in the field of filtration, catalysis, tissue engineering. The use of electrospinning technique is a relatively new route explored for the deposition of organic coatings onto metal substrates with the aim to guarantee active corrosion protection mechanisms together with effective barrier properties, especially for light alloys. PVA is a cheap, widely employed, low environmental impact polymer characterized by chemical resistance, water solubility, and biocompatibility.

The idea was to develop a feasible organic protective layer able to release cerium ions as corrosion inhibitors. For this purpose, electrospun PVA mats made up of nonwoven fibers of 400–500 nm average diameter loaded with different cerium salts have been collected onto aluminium alloy 6082 substrates. After deposition, a low-temperature thermal treatment (120–150°C) has been systematically carried out in order to induce cross-linking reactions and stabilize PVA against dissolution in water. EIS measurements showed that coatings containing cerium (III) acetylacetonate and cerium (III) nitrate cross-linked at 120°C or 150°C, respectively, provided excellent corrosion resistance after 11 days immersion in 3 wt % NaCl solution. It has been also demonstrated that in presence of a damaged coating, cerium (III) acetylacetonate hindered the onset of the corrosion processes and allowed to recover the corrosion resistance value, thus acting as an effective healing agent.

This is a proof-of-concept study that demonstrates the intrinsic potential of the electrospinning technique in the field of advanced polymeric protection coatings. The authors are aware that in order to develop a reliable technological coating, a

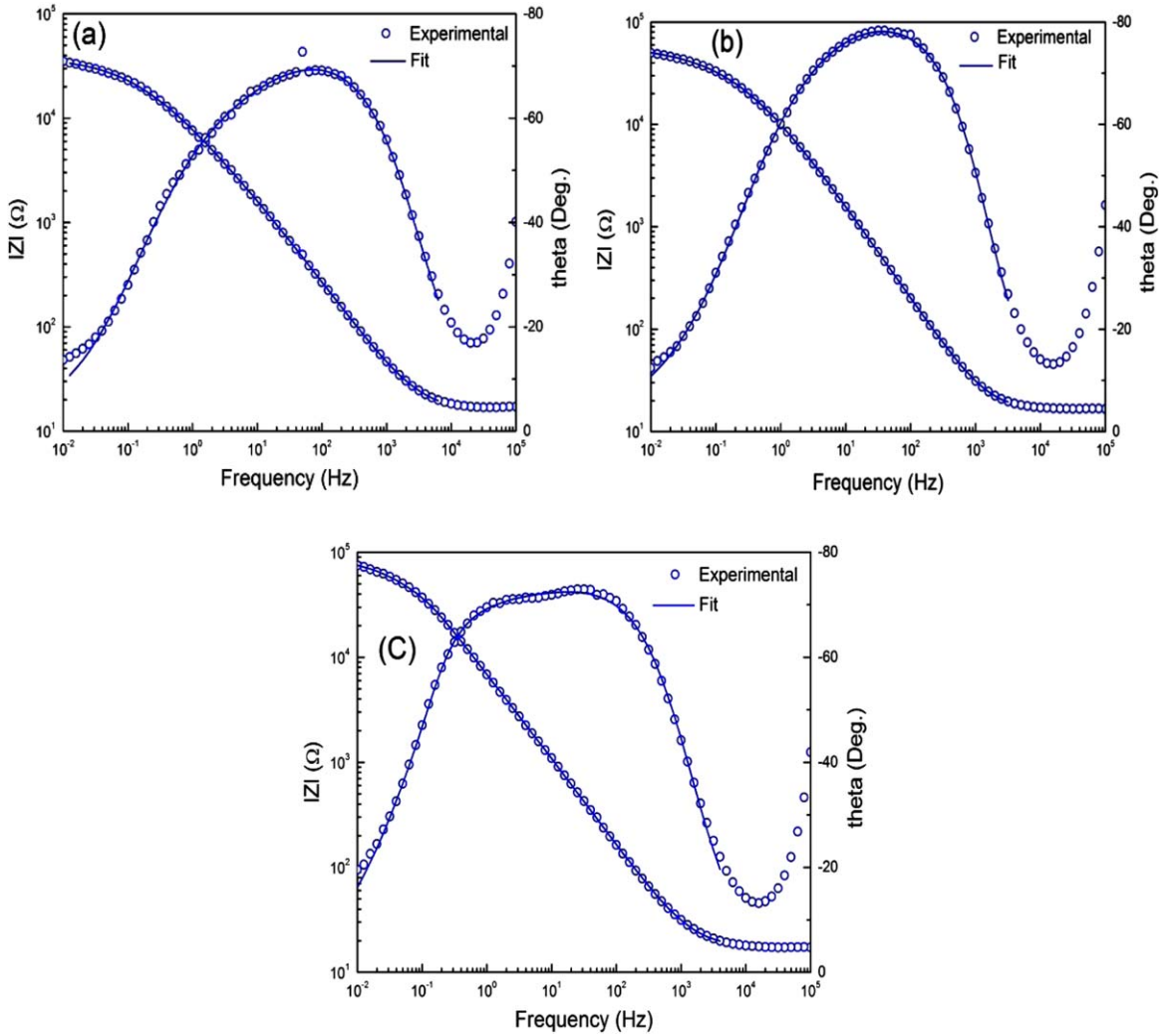

Figure 9. Comparison between EIS experimental data and curve fitting in the Bode representation of (a) intact sample S1, (b) intact sample S4, and (c) damaged sample S1 after 270 h immersion in 3 wt % NaCl solution. [Color figure can be viewed in the online issue, which is available at wileyonlinelibrary.com.]

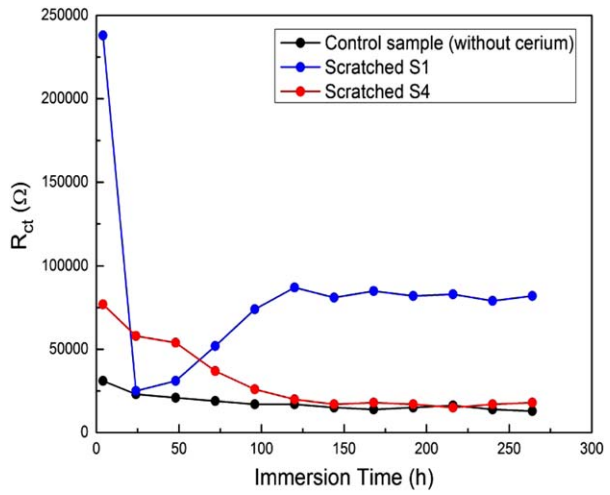

Figure 10. Evolution of the R_{ct} of damaged sample S1, damaged sample S4 and control (without cerium) samples in 3 wt % NaCl solution for 270 h. [Color figure can be viewed in the online issue, which is available at wileyonlinelibrary.com.]

number of points should be in the future further investigated and assessed, referring to both the scale-up of the process and the actual potential of fibrous delivery systems as protective self-healing coatings. The effect of the coating properties on the kinetics of cerium-ions release in terms of thickness, cross-linking degree and crystallinity of the polymeric matrix should be further investigated, especially regarding the difference between organic and inorganic cerium compounds.

Table III. ICP-MS Measurements of Cerium Released in NaCl 3%

Sample	^{140}Ce (μg/L)
NaCl (3 wt %)	< 0.1
S1	0.2
S2	< 0.1
S3	0.1
S4	0.1
Scratched S1	0.5
Scratched S4	0.1

REFERENCES

1. Raps, D.; Hack, T.; Wehr, J.; Zheludkevich, M. L.; Bastos, A. C.; Ferreira, M. G. S.; Nuyken, O. *Corros. Sci.* **2009**, *51*, 1012.
2. Yabuki, A.; Yamagami, H.; Noishiki, K. *Mater. Corros.* **2007**, *58*, 497.
3. Yasakau, K. A.; Zheludkevich, M. L.; Lamaka, S. V.; Ferreira, M. G. S. *J. Phys. Chem. B* **2006**, *110*, 5515.
4. Starke, E. A. Jr.; Staley, *J. T. Prog. Aerosp. Sci.* **1996**, *32*, 131.
5. Lin, S.; Shih, H.; Mansfeld, F. *Corros. Sci.* **1992**, *33*, 1331.
6. Fedrizzi, L.; Deflorian, F.; Bonora, P. L. *Electrochim. Acta* **1997**, *42*, 969.
7. Tallman, D. E.; Pae, Y.; Bierwagen, G. P. *Corrosion* **2000**, *56*, 401.
8. Tallman, D. E.; Vang, C.; Wallace, G. G.; Bierwagen, G. P. *J. Electrochem. Soc.* **2002**, *149*, C173.
9. González-García, Y.; Mol, J. M. C.; Muselle, T.; De Graeve, I.; Van Assche, G.; Scheltjens, G.; Van Mele, B.; Terryn, H. *Electrochem. Commun.* **2011**, *13*, 169.
10. Luo, J. L.; Cui, N. *J. Alloys Compd.* **1998**, *264*, 299.
11. Wu, H. L.; Cheng, Y. L.; Li, L. L.; Chen, Z. H.; Wang, H. M.; Zhang, Z. *Appl. Surf. Sci.* **2007**, *253*, 9387.
12. Guan, H.; Buchheit, R. G. *Corrosion* **2004**, *60*, 284.
13. Wang, C.; Jiang, F.; Wang, F. *Corrosion* **2004**, *60*, 237.
14. Hughes, A. E.; Gorman, J. D.; Miller, P. R.; Sexton, B. A.; Paterson, P. J. K.; Taylor, R. *Surf. Interface Anal.* **2004**, *36*, 290.
15. Yu, Q. S.; Yasuda, H. K. *Prog. Org. Coat.* **2005**, *52*, 217.
16. Palomino, L. E. M.; Aoki, I. V.; de Melo, H. G. *Electrochim. Acta* **2006**, *51*, 5943.
17. Gray, J. E.; Luan, B. *J. Alloys Compd.* **2002**, *336*, 88.
18. Zhong, X.; Li, Q.; Hu, J.; Zhang, S.; Chen, B.; Xu, S.; Luo, F. *Electrochim. Acta* **2010**, *55*, 2424.
19. Jorcin, J. B. et al. *Electrochim. Acta* **2010**, *55*, 6195.
20. Uehara, K.; Ichikawa, T.; Serikawa, T.; Yoshikawa, S.; Ehara, S.; Tsunooka, M. *Thin Solid Films* **1998**, *322*, 198.
21. Feng, W.; Patel, S. H.; Young, M. Y.; Zunino, J. L.; Xanthos, M. *Adv. Polym. Technol.* **2007**, *26*, 1.
22. Wu, D. Y.; Meure, S.; Solomon, D. *Prog. Polym. Sci. (Oxford)* **2008**, *33*, 479.
23. García, S. J.; Fischer, H. R.; Van Der Zwaag, S. *Prog. Org. Coat.* **2011**, *72*, 211.
24. White, S. R.; Sottos, N. R.; Geubelle, P. H.; Moore, J. S.; Kessler, M. R.; Sriram, S. R.; Brown, E. N.; Viswanathan, S. *Nature* **2001**, *409*, 794.
25. Rule, J. D.; Brown, E. N.; Sottos, N. R.; White, S. R.; Moore, J. S. *Adv. Mater.* **2005**, *17*, 205.
26. Cho, S. H.; Andersson, H. M.; White, S. R.; Sottos, N. R.; Braun, P. V. *Adv. Mater.* **2006**, *18*, 997.
27. Blaiszik, B. J.; Sottos, N. R.; White, S. R. *Compos. Sci. Technol.* **2008**, *68*, 978.
28. Chen, X.; Dam, M. A.; Ono, K.; Mal, A.; Shen, H.; Nutt, S. R.; Sheran, K.; Wudl, F. *Science* **2002**, *295*, 1698.
29. Cordier, P.; Tournilhac, F.; Soulié-Ziakovic, C.; Leibler, L. *Nature* **2008**, *451*, 977.
30. Pang, J. W. C.; Bond, I. P. *Compos. Sci. Technol.* **2005**, *65*, 1791.
31. Williams, G.; Trask, R.; Bond, I. *Compos. A Appl. Sci. Manuf.* **2007**, *38*, 1525.
32. Liu, H. A.; Gnade, B. E.; Balkus, K. J. Jr. *Adv. Funct. Mater.* **2008**, *18*, 3620.
33. Park, J. H.; Braun, P. V. *Adv. Mater.* **2010**, *22*, 496.
34. Bethencourt, M.; Botana, F. J.; Calvino, J. J.; Marcos, M.; Rodríguez-Chacón, M. A. *Corros. Sci.* **1998**, *40*, 1803.
35. Twite, R. L.; Bierwagen, G. P. *Prog. Org. Coat.* **1998**, *33*, 91.
36. Davó, B.; De Damborenea, J. J.; *Electrochim. Acta* **2004**, *49*, 4957.
37. Yabuki, A.; Kaneda, R. *Mater. Corros.* **2009**, *60*, 444.
38. Hinton, B. R. W.; Wilson, L. *Corros. Sci.* **1989**, *29*, 967,977.
39. Aldykiewicz, A. J. Jr.; Davenport, A. J.; Isaacs, H. S. *J. Electrochem. Soc.* **1996**, *143*, 147.
40. Lamastra, F. R.; Bianco, A.; Meriggi, A.; Montesperelli, G.; Nanni, F.; Gusmano, G. *Chem. Eng. J.* **2008**, *145*, 169.
41. Shao, C.; Kim, H. Y.; Gong, J.; Ding, B.; Lee, D. R.; Park, S. *J. Mater. Lett.* **2003**, *57*, 1579.
42. Arbelaiz, A.; Fernández, B.; Valea, A.; Mondragon, I. *Carbohydr. Polym.* **2006**, *64*, 224.
43. Yao, L.; Haas, T. W.; Guiseppi-Elie, A.; Bowlin, G. L.; Simpson, D. G.; Wnek, G. E. *Chem. Mater.* **2003**, *15*, 1860.
44. Wutticharoenmongkol, P.; Sanchavanakit, N.; Pavasant, P.; Supaphol, P. *Macromol. Biosci.* **2006**, *6*, 70.
45. Bhardwaj, N.; Kundu, S. C. *Biotechnol. Adv.* **2010**, *28*, 325.
46. Bianco, A.; Federico, E. D.; Moscatelli, I.; Camaioni, A.; Armentano, I.; Campagnolo, L.; Dottori, M.; Kenny, J. M.; Siracusa, G.; Gusmano, G. *Mater. Sci. Eng. C* **2009**, *29*, 2063.
47. Deitzel, J. M.; Kosik, W.; McKnight, S. H.; Beck Tan, N. C.; DeSimone, J. M.; Crette, S. *Polymer* **2002**, *43*, 1025.
48. Ding, B.; Kim, H.-Y.; Lee, S.-C.; Shao, C.-L.; Lee, D.-R.; Park, S.-J.; Kwag, G.-B.; Cho, K.-J. *J. Polym. Sci. B Polym. Phys.* **2002**, *40*, 1261.
49. Blanes, M.; Gisbert, M. J.; Marco, B.; Bonet, M.; Gisbert, J.; Balart, R.*Text. Res. J.* **2010**, *80*, 1465.
50. Park, J. S.; Park, J. W.; Ruckenstein, E. *J. Appl. Polym. Sci.* **2001**, *82*, 1824.
51. Zhang, Y.; Zhu, P. C.; Edgren, D. *J. Polym. Res.* **2010**, *17*, 725.
52. Panzavolta, S.; Gioffrè, M.; Focarete, M. L.; Gualandi, C.; Foroni, L.; Bigi, A. *Acta Biomater.* **2011**, *7*, 1702.
53. Qiu, K.; Netravali, A. N. *Compos. Sci. Technol.* **2012**, *72*, 1588.
54. Mehta, N. K.; Bogere, M. N. *Prog. Org. Coat.* **2009**, *64*, 419.
55. Lamaka, S. V.; Zheludkevich, M. L.; Yasakau, K. A.; Serra, R.; Poznyak, S. K.; Ferreira, M. G. S. *Prog. Org. Coat.* **2007**, *58*, 127.
56. Bagalà, P.; Lamastra, F. R.; Kaciulis, S.; Mezzi, A.; Montesperelli, G. *Surf. Coat. Technol.* **2012**, *206*, 4855.
57. Wang, H.; Akid, R.; Gobara, M. *Corros. Sci.* **2010**, *52*, 2565.
58. Bonora, P. L.; Deflorian, F.; Fedrizzi, L. *Electrochim. Acta* **1996**, *41*, 1073.
59. Zhong, X.; Li, Q.; Hu, J.; Lu, Y. *Corros. Sci.* **2008**, *50*, 2304.